Bioorganic Chemistry 90 (2019) 103077

Contents lists available at ScienceDirect

Bioorganic Chemistry

journal homepage: www.elsevier.com/locate/bioorg

5,6,7,8-Tetrahydrobenzo[4,5]thieno[2,3-*d*]pyrimidine derivatives as inhibitors of full-length RORγt

Chuyu Lao[1], Xiaoqing Zhou[1], Huanpeng Chen, Fengjiao Wei, Zhaofeng Huang*, Chuan Bai*

Institute of Human Virology, Guangdong Engineering Research Center for Antimicrobial Agent and Immunotechnology, Zhongshan School of Medicine, Sun Yat-sen University, Guangzhou, Guangdong 510080, China

ARTICLE INFO

Keywords:
RORγt
Th17
Inhibitor

ABSTRACT

Retinoid-related orphan receptor gamma-t (RORγt) belongs to the nuclear receptor superfamily that takes vital roles in the development and maturation of *T*-helper 17 cell (Th17) and lymph-node genesis. Because Th17 cells have been proved to be major effectors in human autoimmune and inflammatory diseases, the agonists and antagonists of RORγt have been discovered as promising leads for the therapeutics of these diseases. Most of the current studies of RORγt inhibitors have been focused on ligand binding domain (LBD) of RORγt because the structure and binding pockets of LBD have been elucidated and studied in detail. Recent research elucidated that the hinge domain (HD) of RORγt was significantly involved in the SUMOylation of RORγt and thus specifically affecting T cell development but not lymph-node genesis. These discoveries highlighted the potential of HD of RORγt as the target of RORγt inhibitors that could specifically inhibit Th17-related activities without affecting lymph-node genesis. In this study, we utilized a screening system with full-length RORγt including DBD, HD and LBD to evaluate the activities of a synthesized library of tetrahydrobenzo[4,5]thieno[2,3-*d*]pyrimidine derivatives. We identified a potent lead compound (**28**) that effectively inhibited Th17 cell differentiation. Docking and structure–activity relationship (SAR) studies showed that compound **28** may not bind in the binding pocket as most of the known inhibitors, but may bind in the pocket closed to Gln223 and Leu244 in HD. Our studies showed evidence that the HD of RORγt could afford a binding pocket for Th17 specific inhibitors and this domain should be further studied to discover potent and specific RORγt inhibitors.

1. Introduction

Retinoid-related orphan receptor gamma-t (RORγt) is a crucial transcription factor for the regulations of differentiation of the Th17 subset of helper T cells [1–3]. RORγt has been studied as a promising target to develop therapeutics for autoimmune inflammation diseases including multiple sclerosis (MS) and psoriasis because Th17 cells take important roles in these diseases [3–10]. Based on the wealth of structural and biological data of RORγt LBD, many modulators targeting RORγt LBD have been discovered and some of them have been in the clinical trials [11–22]. The binding pockets of these modulators mainly belong to two categories: the digoxin binding site and the pocket closed to H12 [23–26]. The modulators binding in the digoxin site mostly could compete with digoxin and showed inhibitory effect [23]. The modulators targeting the second binding site could work as agonists or antagonists according to their specific interactions with the key amino acid residues of LBD [25]. An allosteric binding site of RORγt binding closed to H12 in LBD has also been discovered [27].

Besides the function to modulate Th17 cell differentiation, RORγt also plays vital roles in thymocyte development and lymph-node genesis, which have been showed to be related with the side effects of some RORγt inhibitors [28–31]. The ideal RORγt inhibitors should only be active to inhibit Th17 cell differentiation without affecting the thymocyte development. Recent studies discovered that the mutations of key amino acid residues on HD of RORγt, such as serine at position 92 and leucine at position 93, abolished RORγt's function in Th17 differentiation but not in thymocyte development [32,33]. These results indicated that the HD could be a target to modulate only Th17-related functions of RORγt. Herein, we designed and synthesized a library consisted of tetrahydrobenzo[4,5]thieno[2,3-*d*]pyrimidine derivatives and evaluated their activities with a screening system composed by full-length RORγt protein including LBD, HD and DBD [34,35]. Then the inhibitory activities of the hit compounds on Th17 cell differentiation and IL-17 production were evaluated in splenic naive CD4+ T cells.

* Corresponding authors at: Sun Yat-sen University, 74 Zhongshan 2nd Road, Guangzhou 510080, China.
E-mail addresses: hzhaof@mail.sysu.edu.cn (Z. Huang), baichuan@mail.sysu.edu.cn (C. Bai).
[1] These authors contributed equally to this work.

https://doi.org/10.1016/j.bioorg.2019.103077
Received 25 April 2019; Received in revised form 12 June 2019; Accepted 17 June 2019
Available online 21 June 2019
0045-2068/

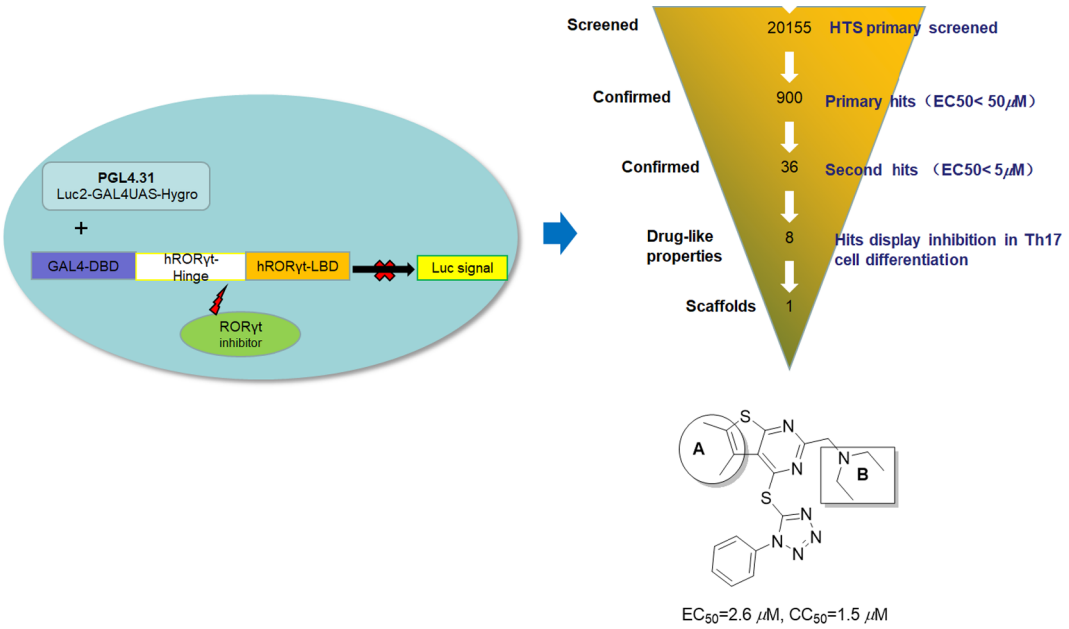

Scheme 1. The hit compound as a RORγt inhibitor was discovered in a HTS targeting full-length RORγt. In this work, the SAR of hit was performed in Part A (circle) and B (rectangle).

Our results showed that the tetrahydrobenzo[4,5]thieno[2,3-*d*]pyrimidine could be an active skeleton structure to discover and develop RORγt inhibitors with potent Th-17 specific activities.

2. Results and discussions

2.1. Chemistry

In the previous study of RORγt inhibitors, we discovered the hit compound with thieno[2,3-*d*]pyrimidine structure [35]. In this study, we synthesized compounds with modifications on Part A and B to study the structure–activity relationship (SAR) in detail (Scheme 1).

To expand the chemical diversity of Part A, we first introduced cyclohexane structure on thiophene moiety. The alky or halogen substitutions on the cyclohexane structure of Part A were installed to afford key intermediate **2** (Scheme 2). We also introduced carboxylic acid group (**14**) on the cyclohexane structure to afford more chemical diversity by the convenient amide synthesis (Scheme 3).

To study the SAR of Part B, we used compound **2** to prepare the key intermediate **26** and then installed substitution groups by ester or amide synthesis (Scheme 4).

2.2. SAR studies of Part A

First we installed cyclohexane group on Part A and this compound **6** (Table 1) showed similar inhibitory activity with the hit compound (EC_{50}: 2.60 μM for hit vs 2.79 μM for compound **6**). Then we try to study whether alky modifications on Part A could afford better activities. The compounds with methyl (**7**), ethyl (**8**) and propyl (**9**) groups were inactive and the compounds with di-alkyl groups (**10** and **11**) afforded lower activity than the hit compound. Then we installed electro-withdrawing groups such as fluorine (**12**), ester groups (**13**), and carboxylic acid (**14**) on Part A and compound **12** showed the more potent inhibitory activity but higher cytotoxicity than compound **6**.

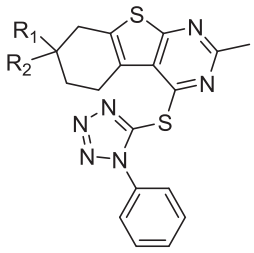

Because the ester group on part A (**13**) showed similar activity and better cytotoxicity compared with compound **6**, we then synthesized compounds with amide groups in this part (Table 2). The non-polar tetrahydropyran group (**15**) and alkyl-substituted phenyl groups (**16**, **17**) totally abolished the activity. Compound **18** with benzyl group showed weaker activity than compound **6**. Then we tried to install chlorine (**19**) and bromine (**20**) substituted phenyl groups but did not achieve better activity. In the next, we postulated that the heterocycles may have some advantages by forming H-bonds or electrostatic interactions in the binding site. So we synthesized compounds with thiazole (**21**) and 5-methyl-thiazole (**22**) groups. Although compound **21** did not show strong activity, the very similar compound **22** showed similar inhibitory activity with compound **6**. We then installed larger heterocycles (**23–25**), but they were much less active than compound **6**, which indicated that the steric hindrance may have adverse effect for their binding.

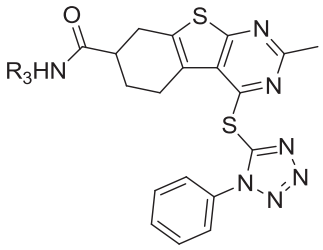

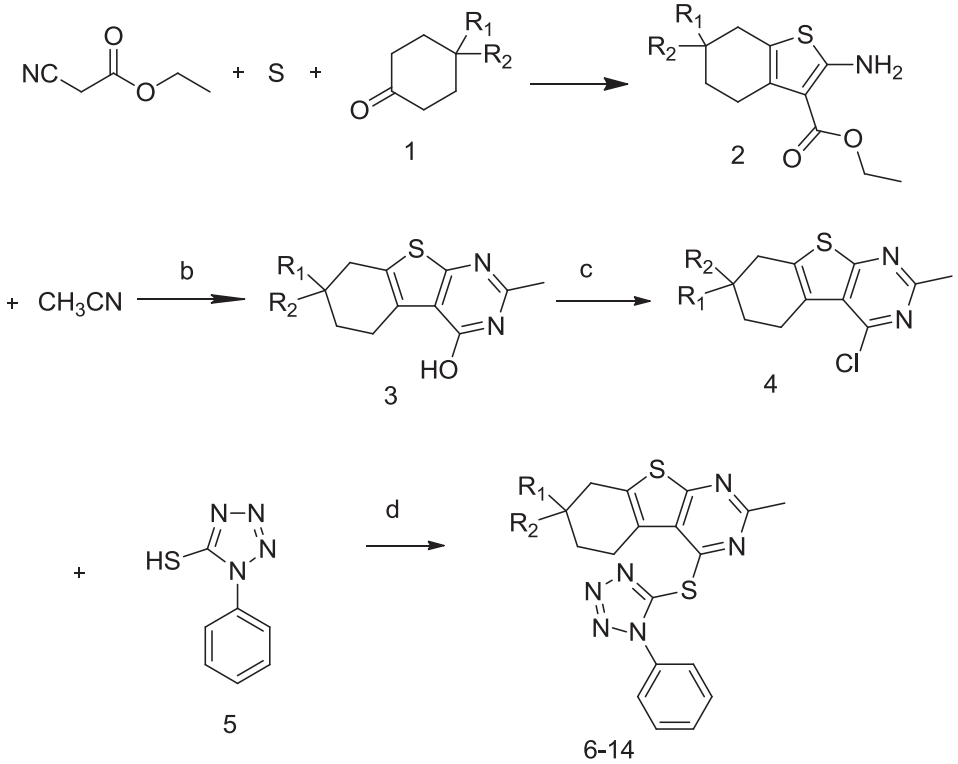

Scheme 2. Synthesis of compounds with alky or halogen modifications on Part A. Reagents and conditions: (a) Morpholine, E_tOH, 60 °C; (b) 4 N HCl in 1,4-dioxane, 100 °C; (c) $POCl_3$, 110 °C reflux; (d) $NaHCO_3$, DMSO, 80 °C.

2.3. SAR studies of part B

The results of SAR studies of Part A indicated that the binding pocket may be relatively strict for the volume of the Part A. Thereof, we next evaluated the effects of the groups on C-2 of pyrimidine of Part B on the activity. The carboxylic acid group (**29**) abolished the inhibitory activity. However, compound **28** with ester group showed best activities and highest CC_{50}/EC_{50} ratio (22). Then we installed relatively larger heterocycles on part B. Compound **31** with benzoimidazole group also showed better inhibitory activity and cytotoxicity than compound **6** (see Table 3).

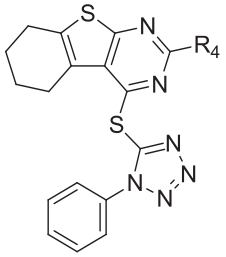

2.4. Biological activities and working mechanism

In the SAR studies of the synthesized thieno[2,3-*d*]pyrimidine derivatives with the cell-based ROR reporter luciferase assay, compounds **6**, **10**, **22**, **28** and **31** showed potent inhibitory activities. Thereof, we further investigated their inhibitory activities on Th17 differentiation in splenic naive CD4 + T cells from C57BL/6J mice (Fig. 1). Compound **28** showed the best activity to inhibit Th17 differentiation at 3.12 μM without obvious toxicities.

Besides IL-17 production and Th17 differentiation, RORγt has been also involved in multiple pathway in immunology and cancer development, so the desired inhibitor should avoid decreasing RORγt level while specifically inhibit RORγt's activity. Thereof, we studied the inhibitory effects of compound **6**, **10**, **22**, **28** and **31** on the production of IL-17A and IL-17F, together with their effects on RORγt mRNA level (Fig. 2). Compound **28** inhibited both IL-17A and IL-17F production in a dose-dependent way and showed best activity at 6.25 μM. Meanwhile, we also tested whether compound **6**, **10**, **22**, **28** and **31** would affect the apoptosis of PGL4.31 + hRORγt + Jurkat cells and thymocytes. Only compound **10** slightly increased apoptosis compared to control. All compounds except compound **22** could affect only about 10% of thymocyte survival (Figs. S3 and S4).

To elucidate the working mechanism of compound **28** on RORγt, it

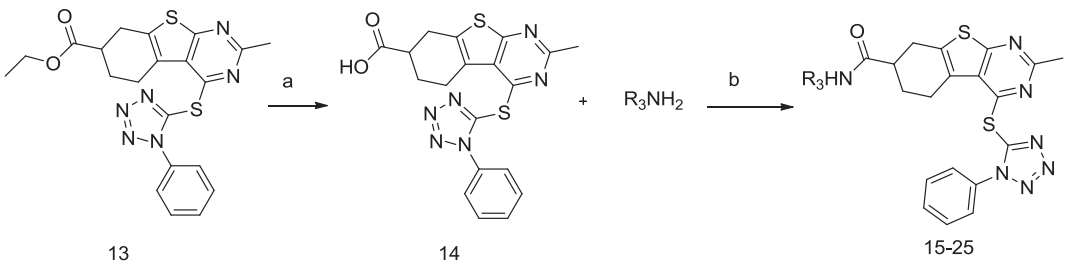

Scheme 3. Synthesis of compounds with amide modifications on Part A. Reagents and conditions: (a) 1 N LiOH, RT; (b) HOBT, EDCI, DCM, RT.

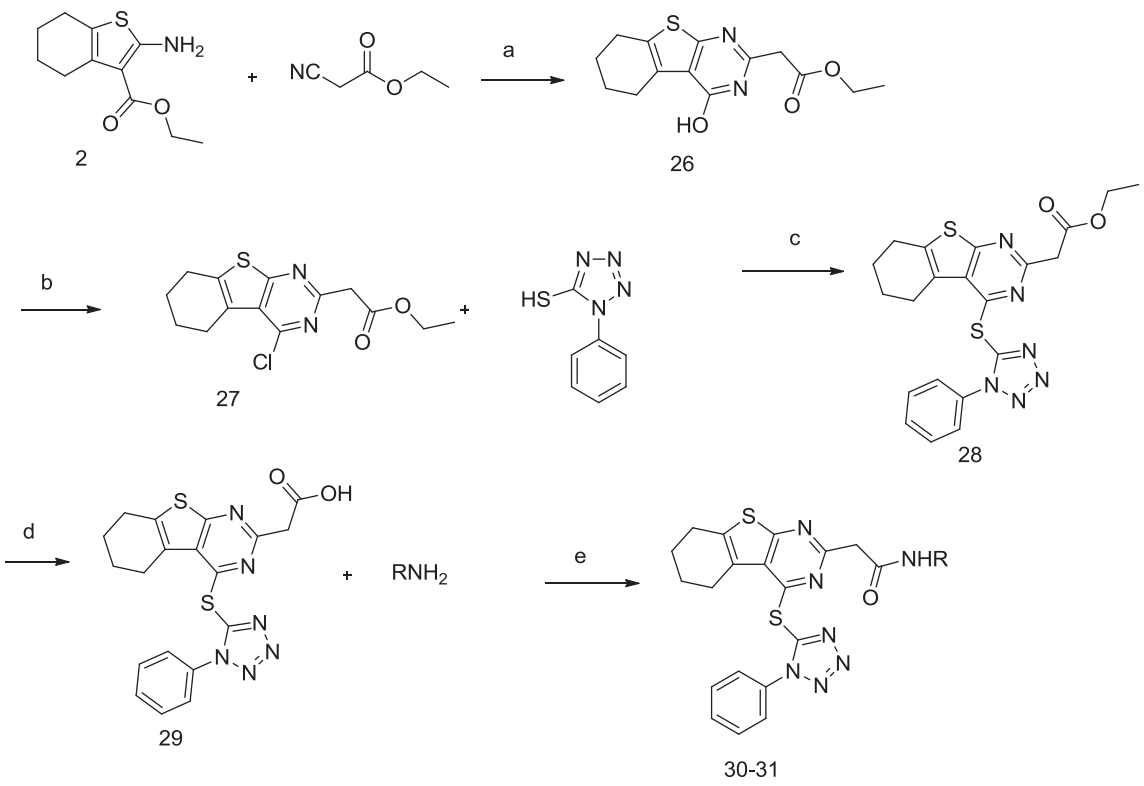

Scheme 4. Synthesis of compounds with modifications on Part B. Reagents and conditions: (a) 4 N HCl in 1,4-dioxane, 100 °C; (b) $POCl_3$, 110 °C reflux; (c) $NaHCO_3$, DMSO, 80 °C; (d) 1 N LiOH, RT; (e) HOBT, EDCI, DCM, RT.

Table 1
The SAR studies of Part A.

Compd. No.	R_1	R_2	EC_{50}[a] (μM)	CC_{50}[b] (μM)	clogP[c]
6	H	H	2.79	3.98	4.01
7	Me	H	> 10	> 10	4.25
8	Et	H	> 10	> 10	4.46
9	Pro	H	> 10	> 10	5.03
10	Me	Me	4.58	7.70	4.64
11	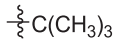	H	8.25	< 1	4.64
12	F	F	1.35	< 1	3.96
13	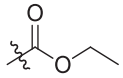	H	6.15	> 10	3.80
14		H	> 20	> 10	3.32

[a] EC_{50} (μM), half maximal (50%) effective concentration against PGL4.31 + hRORγt + Jurkat cells.
[b] CC_{50} (μM), median (50%) cytotoxic concentration in PGL4.31 + hRORγt + Jurkat cells.
[c] clogP was calculated by LigandScout 4.2.

is important to understand the binding model of compound **28** in RORγt protein. We first studied the binding affinity of compound **28** with RORγt protein with SPR (Fig. 3A). The SPR studies showed that compound **28** bond with RORγt protein. Considering that our assay system that utilized the full-length RORγt protein but not LBD of RORγt, we then conducted the docking study to test whether the full-length RORγt would afford novel binding model of compound **28**. We first built a model (I-TASSER) of full-length RORγt protein due to the lack of the crystal structure of full-length RORγt (Fig. 3B). The docking experiments showed that RORγt may not bind in the known binding site closed to H12 of RORγt (Fig. 3C), but it may bind in the pocket composed by the amino acids from hinge domain, in which compound **28** may form electrostatic interaction with Gln223 and hydrophobic interaction with Leu244 (Fig. 3D).

3. Experimental

3.1. Chemistry

All chemicals were purchased from commercial vendors and used without further purification. All reactions requiring anhydrous conditions were carried out under argon or nitrogen atmosphere using oven-dried glassware. All NMR spectra (^{1}H NMR, ^{13}C NMR) were recorded on Bruker 400 MHz/500 MHz NMR spectrometers, using TMS as an internal standard. Chemical shifts are reported in parts per million referenced with respect to appropriate internal standards or residual solvent peaks. Mass spectral data (ESI) were gathered on Thermofisher LCQ Mass spectrometry.

3.1.1. Procedure for the preparation of compound *2*

4-Cyclohexanone derivatives (**1**) (5.50 mmol) and morpholine (5.50 mmol) was added to the mixture of ethyl cyanoacetate (5.01 mmol) and sulfur (5.50 mmol). Then the mixture was dissolved in ethanol (5 mL) and stirred at 60 °C for 16 h. The reaction mixture was cooled to room temperature and the solvents were removed in vacuo. The crude product was purified by flash column chromatography on a silica column using c-hexane/ethyl acetate (50:1) as the eluent to get compound **2** (95% yield) as a white/yellow solid.

3.1.2. Procedure for the preparation of compound *3* and compound *26*

Compound **2** (3.53 mmol) was dissolved in acetonitrile (5 mL) or ethyl cyanoacetate (5 mL) was added 4 N HCl in 1,4-dioxane (4 mL) and the mixture was stirred at 100 °C overnight. The mixture was cooled to room temperature and the solvents were removed in vacuo. The residue was dissolved in ethyl acetate. Subsequently, saturated aqueous $NaHCO_3$ was added to the mixture and after extracted with ethyl

Table 2
The SAR studies of Part A with amide groups.

Compd. No.	R_3	EC_{50}[a] (μM)	CC_{50}[b] (μM)	clogP[c]
15	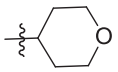	> 10	< 10	3.53
16	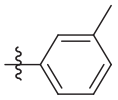	> 10	< 10	5.18
17	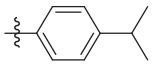	> 10	< 1	5.99
18	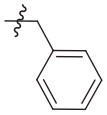	12.60	> 10	4.26
19	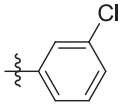	> 10	< 10	5.52
20	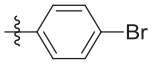	> 10	< 10	5.63
21		> 10	< 10	4.33
22	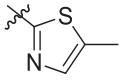	9.06	4.32	4.64
23	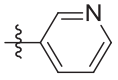	> 10	< 5	4.27
24	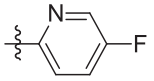	> 10	< 10	4.40
25	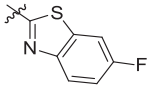	> 10	< 5	5.62

Table 3
The SAR studies of Part B.

Compd. No.	R_4	EC_{50}[a] (μM)	CC_{50}[b] (μM)	clogP[c]
28	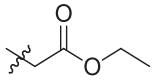	0.14	3.35	3.80
29	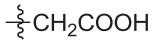	> 10	> 10	3.32
30	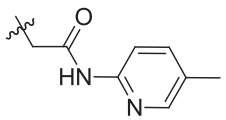	> 10	4.014	4.58
31	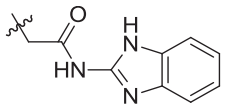	0.85	9.176	4.76

acetate. The extract was washed with brine and dried to give compound **3** or compound **26** (75% yield) as white/yellow solid.

*3.1.3. Procedure for the preparation of compound **4** and compound **27***

To a solution of compound **3** (0.82 mmol) or compound **26** (0.82 mmol) in phosphorus oxychloride (5 mL) was refluxed at 110 °C for 3 h. The mixture was cooled to room temperature and the solvents were removed in vacuo. The residue was dissolved in ethyl acetate. Subsequently, saturated aqueous $NaHCO_3$ was added to the mixture and after extracted with ethyl acetate. The extract was washed with brine and dried to get compound **4** or compound **27** (97% yield) without purification as white solid.

*3.1.4. Procedure for the preparation of compound **5***

To a solution of phenyl isothiocyanate (2700 mg, 20.00 mmol) and sodium azide (1952 mg, 30.04 mmol) in H_2O (20 mL) was stirred at 90 °C for 16 h. The mixture was cooled to room temperature and extracted with ethyl acetate to remove the byproducts. The aqueous phase was neutralized with 1 N HCl and extracted with ethyl acetate. The organic phase was washed with brine and the solvents was removed in vacuo to get compound **5** (75% yield) without purification as white solid.

*3.1.5. Procedure for the preparation of compound **6–13** and compound **28***

To a solution of compound **4** (0.65 mmol) or compound **27**, compound **5** (0.73 mmol) and sodium bicarbonate (1.30 mmol) in DMSO (5 mL) was stirred at 80 °C for 16 h. The mixture was extracted with ethyl acetate. The extract was washed with saline and the solvents were removed in vacuo. The crude product was purified by silica gel chromatography using cyclohexane-ethyl acetate(25:1) as eluate to give compound **6–13** or compound **28** (63% yield) as white solid.

2-Methyl-4-((1-phenyl-1H-tetrazol-5-yl)thio)-5,6,7,8-tetrahydrobenzo [4,5]thieno[2,3-d]pyrimidine **(6)**. Yield = 36%; ^{1}H NMR (500 MHz, $CDCl_3$) δ 7.63 (dt, J = 8.4, 3.6 Hz, 2H), 7.55–7.44 (m, 3H), 3.04 (t, J = 4.8 Hz, 2H), 2.86 (d, J = 5.2 Hz, 2H), 2.45 (s, 3H), 1.99–1.88 (m, 4H), 1.28 (s, 1H). ^{13}C NMR (126 MHz, $CDCl_3$) δ 167.74 (s), 161.14 (s), 155.98 (s), 146.50 (s), 137.61 (s), 134.23 (s), 130.44 (s), 129.40 (s), 125.90 (d, J = 14.9 Hz), 124.53 (s), 29.70 (s), 26.07 (s), 25.72 (s), 25.21 (s), 22.42 (d, J = 12.8 Hz). ESI-MS m/z: 381.2 $[M + H]^+$.

2,7-Dimethyl-4-((1-phenyl-1H-tetrazol-5-yl)thio)-5,6,7,8-tetrahydrobenzo[4,5]thieno[2,3-d]pyrimidine **(7)**. Yield = 7%; ^{1}H NMR (500 MHz, DMSO) δ 7.69 (dd, J = 7.7, 1.8 Hz, 2H), 7.58–7.44 (m, 3H), 3.13–3.00 (m, 1H), 2.90 (dd, J = 17.0, 4.5 Hz, 2H), 2.41 (dd, J = 17.9, 10.3 Hz, 1H), 2.36 (s, 3H), 1.93 (s, 2H), 1.52–1.42 (m, 1H), 1.05 (d, J = 6.5 Hz, 3H). ^{13}C NMR (126 MHz, DMSO) δ 167.38 (s), 161.09 (s), 156.58 (s), 147.59 (s), 137.40 (s), 134.03 (s), 131.13 (s), 129.97 (s), 125.96 (s), 125.44 (s), 33.37 (s), 30.28 (s), 28.68 (s), 25.76 (s), 25.36 (s), 21.39 (s). ESI-MS m/z: 395.10 $[M + H]^+$.

7-Ethyl-2-methyl-4-((1-phenyl-1H-tetrazol-5-yl)thio)-5,6,7,8-tetrahydrobenzo[4,5]thieno[2,3-d]pyrimidine **(8)**. Yield = 39%; ^{1}H NMR (500 MHz, $CDCl_3$) δ 7.64–7.57 (m, 2H), 7.50–7.42 (m, 3H), 3.17 (dd, J = 10.6, 8.2 Hz, 1H), 2.98–2.86 (m, 2H), 2.49–2.43 (m, 1H), 2.42 (s, 3H), 2.12–2.04 (m, 1H), 1.82–1.70 (m, 1H), 1.55–1.38 (m, 3H), 0.99 (t, J = 7.4 Hz, 3H). ^{13}C NMR (126 MHz, $CDCl_3$) δ 167.90 (s), 161.13 (s), 155.98 (s), 146.52 (s), 137.45 (s), 134.21 (s), 130.47 (s), 129.43 (s), 125.89 (s), 124.55 (s), 35.62 (s), 31.66 (s), 28.40 (d, J = 20.6 Hz), 28.31–28.13 (m), 25.85 (s), 25.24 (s), 11.44 (s). ESI-MS m/z: 409.26 $[M + H]^+$.

2-Methyl-4-((1-phenyl-1H-tetrazol-5-yl)thio)-7-propyl-5,6,7,8-tetrahydrobenzo[4,5]thieno[2,3-d]pyrimidine **(9)**. Yield = 41%; ^{1}H NMR (500 MHz, DMSO) δ 7.69 (dd, J = 7.6, 1.9 Hz, 2H), 7.56–7.46 (m, 3H), 3.07 (d, J = 16.0 Hz, 1H), 2.95–2.82 (m, 2H), 2.42 (dd, J = 17.2, 9.9 Hz, 1H), 2.35 (s, 3H), 1.99 (d, J = 13.5 Hz, 1H), 1.80 (s, 1H), 1.46 (ddd, J = 23.8, 10.8, 5.8 Hz, 1H), 1.41–1.29 (m, 4H), 0.90 (t, J = 6.8 Hz, 3H). ^{13}C NMR (126 MHz, DMSO) δ 167.40 (s), 161.08 (s), 156.54 (s), 147.58 (s), 137.54 (s), 134.03 (s), 131.13 (s), 129.97 (s), 126.19 (s), 125.44 (s), 37.83 (s), 33.33 (s), 31.67 (s), 28.46 (s), 25.77 (s), 25.37 (s), 19.90 (s), 14.61 (s). ESI-MS m/z: 423.21 $[M + H]^+$.

2,7,7-Trimethyl-4-((1-phenyl-1H-tetrazol-5-yl)thio)-5,6,7,8-tetrahydrobenzo[4,5]thieno[2,3-d]pyrimidine **(10)**. Yield = 28%; ^{1}H NMR (500 MHz, CDCl3) δ 7.65–7.59 (m, 2H), 7.51–7.44 (m, 3H), 3.02 (t,

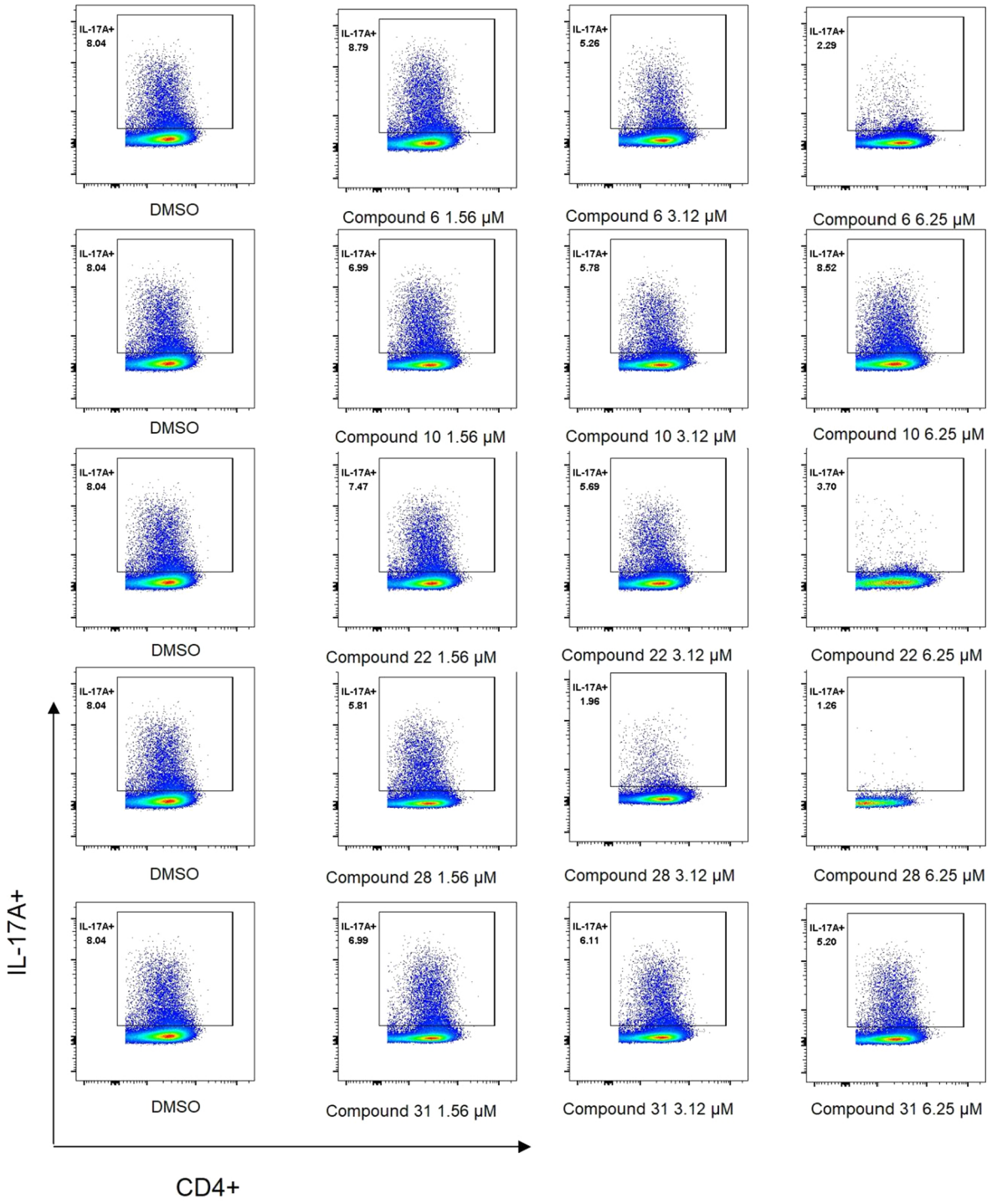

Fig. 1. Compound **6, 10, 22, 28** and **31** inhibited Th17 differentiation. Splenic naive CD4 + T cells from C57BL/6J mice were differentiated *in vitro* into Th17 cells. (A–F) Flow cytometry plots of the percent of IL-17A-expressing CD4 + T cells differentiated under Th17 cell conditions in the presence of different concentration of five compounds. The *in vitro* differentiation was repeated 3 times with consistent results.

J = 6.4 Hz, 2H), 2.62 (d, J = 15.9 Hz, 2H), 2.45 (d, J = 20.8 Hz, 3H), 2.16 (d, J = 12.3 Hz, 1H), 1.76–1.54 (m, 4H), 1.44–1.40 (m, 1H), 1.37 (s, 1H), 1.33 (s, 1H), 1.24 (dd, J = 24.2, 13.0 Hz, 4H), 1.06 (s, 6H). ^{13}C NMR (126 MHz, CDCl3) δ 167.92 (s), 161.11 (s), 156.08 (s), 146.55 (s), 137.11 (s), 134.20 (s), 130.49 (s), 129.44 (s), 125.66 (s), 124.60 (s), 39.14 (s), 35.16 (s), 31.48 (d, J = 8.8 Hz), 30.51–29.31 (m), 29.39–29.31 (m), 27.70 (s), 25.24 (s), 23.85 (s). ESI-MS *m/z*: 409.15 $[M + H]^+$.

7-(Tert-butyl)-2-methyl-4-((1-phenyl-1H-tetrazol-5-yl)thio)-5,6,7,8-tetrahydrobenzo[4,5]thieno[2,3-d]pyrimidine **(11)**. Yield = 31%; ^{1}H NMR (500 MHz, $CDCl_3$) δ 7.60 (dd, J = 6.4, 3.0 Hz, 2H), 7.45 (dd, J = 7.2, 3.6 Hz, 3H), 3.24 (dd, J = 16.1, 4.9 Hz, 1H), 2.85 (td, J = 16.5, 5.2 Hz, 2H), 2.62–2.53 (m, 1H), 2.42 (s, 3H), 2.18–2.13 (m, 1H), 1.58 (ddd, J = 11.8, 4.5, 3.0 Hz, 1H), 1.43 (ddd, J = 24.7, 12.3, 5.1 Hz, 1H), 0.96 (s, 9H). ^{13}C NMR (126 MHz, CDCl3) δ 167.95 (s), 161.12 (s), 155.89 (s), 146.50 (s), 138.40 (s), 134.18 (s), 130.48 (s), 129.43 (s), 125.93 (s), 125.57 (s), 124.52 (s), 44.52 (s), 32.51 (s), 27.22 (t, J = 18.6 Hz), 25.27 (s), 24.05 (s). ESI-MS *m/z*: 437.26 $[M + H]^+$.

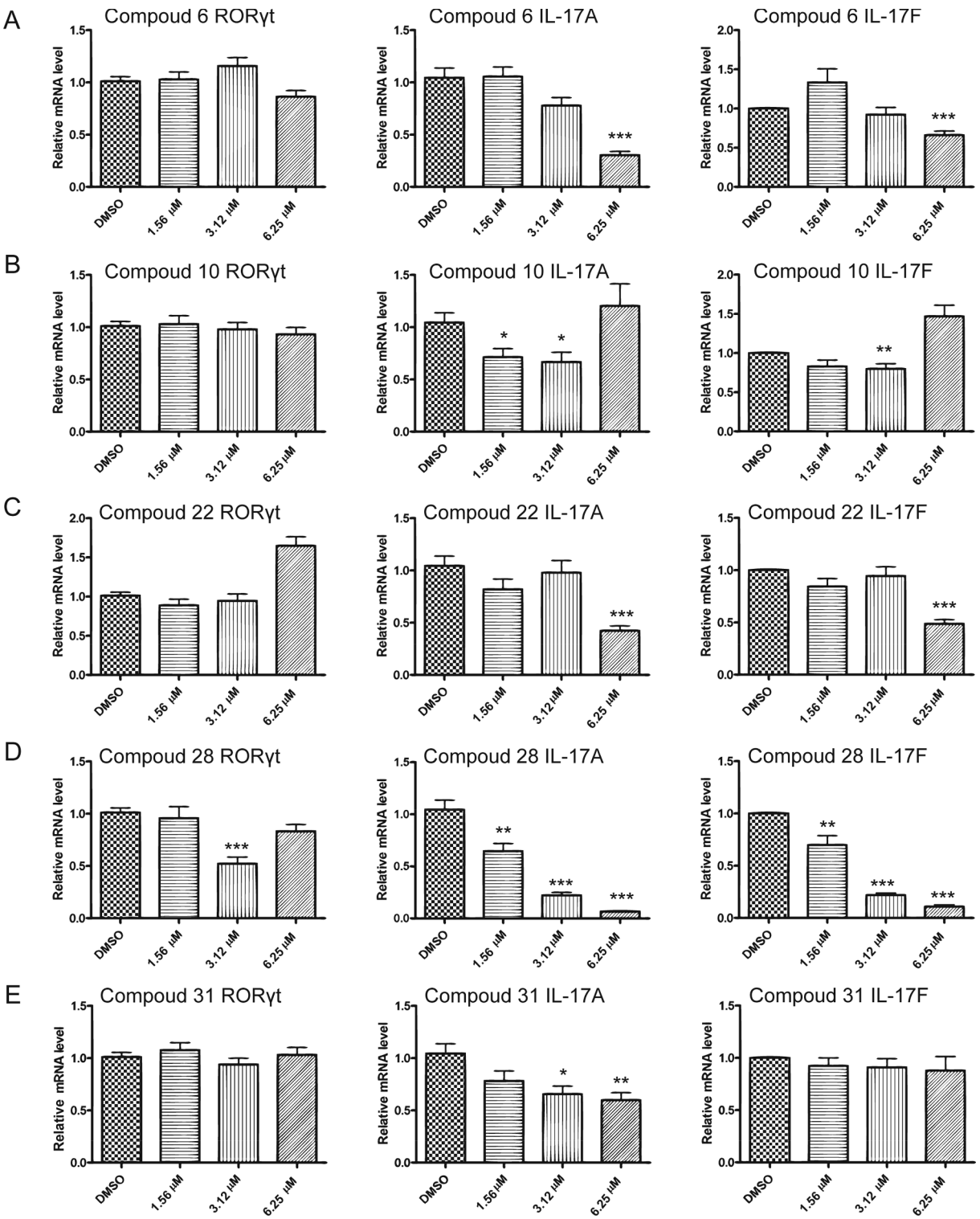

Fig. 2. The effects on expression of cytokines under Th17 cell conditions after treated with compound **6, 10, 22, 28** and **31**. (A–F) The mRNA expression levels of RORγt, IL-17A and IL-17F under Th17 cell conditions. RORγt, IL-17A and IL-17F expression was quantified and normalized to GAPDH. The Q-PCR data were repeated 3 times with consistent results. The results are shown as mean ± SEM; $^{*}p < 0.05$; $^{**}p < 0.01$; $^{***}p < 0.001$.

7,7-Difluoro-2-methyl-4-((1-phenyl-1H-tetrazol-5-yl)thio)-5,6,7,8-tetrahydrobenzo[4,5]thieno[2,3-d]pyrimidine **(12)**. Yield = 35%; ^{1}H NMR (500 MHz, $CDCl_3$) δ 7.63–7.57 (m, 2H), 7.51–7.43 (m, 3H), 3.34 (ddd, J = 30.6, 12.3, 4.6 Hz, 4H), 2.36 (ddd, J = 20.1, 13.4, 6.6 Hz, 2H). ^{13}C NMR (126 MHz, DMSO) δ 167.97 (s), 161.71 (s), 157.22 (s), 147.50 (s), 133.95 (s), 131.13 (s), 129.97 (s), 125.41 (s), 124.77 (s), 124.52 (s), 34.97 (d, J = 28.7 Hz), 34.76–34.65 (m), 34.62 (s), 29.94 (s), 29.65 (d, J = 24.2 Hz), 29.41–29.18 (m), 25.39 (s), 23.86 (s). ESI-MS *m/z*: 417.14 $[M + H]^+$.

Ethyl-2-methyl-4-((1-phenyl-1H-tetrazol-5-yl)thio)-5,6,7,8-tetrahydrobenzo[4,5]thieno[2,3-d]pyrimidine-7-carboxylate **(13)**. Yield = 78%;^{1}H NMR (500 MHz, CDCl3) δ 7.63–7.57 (m, 2H), 7.52–7.44 (m, 3H), 4.20 (q, J = 7.1 Hz, 2H), 3.20 (ddd, J = 16.3, 5.3, 4.4 Hz, 1H), 3.09 (d, J = 6.5 Hz, 2H), 3.07–2.96 (m, 1H), 2.92–2.80 (m, 1H), 2.41 (d,

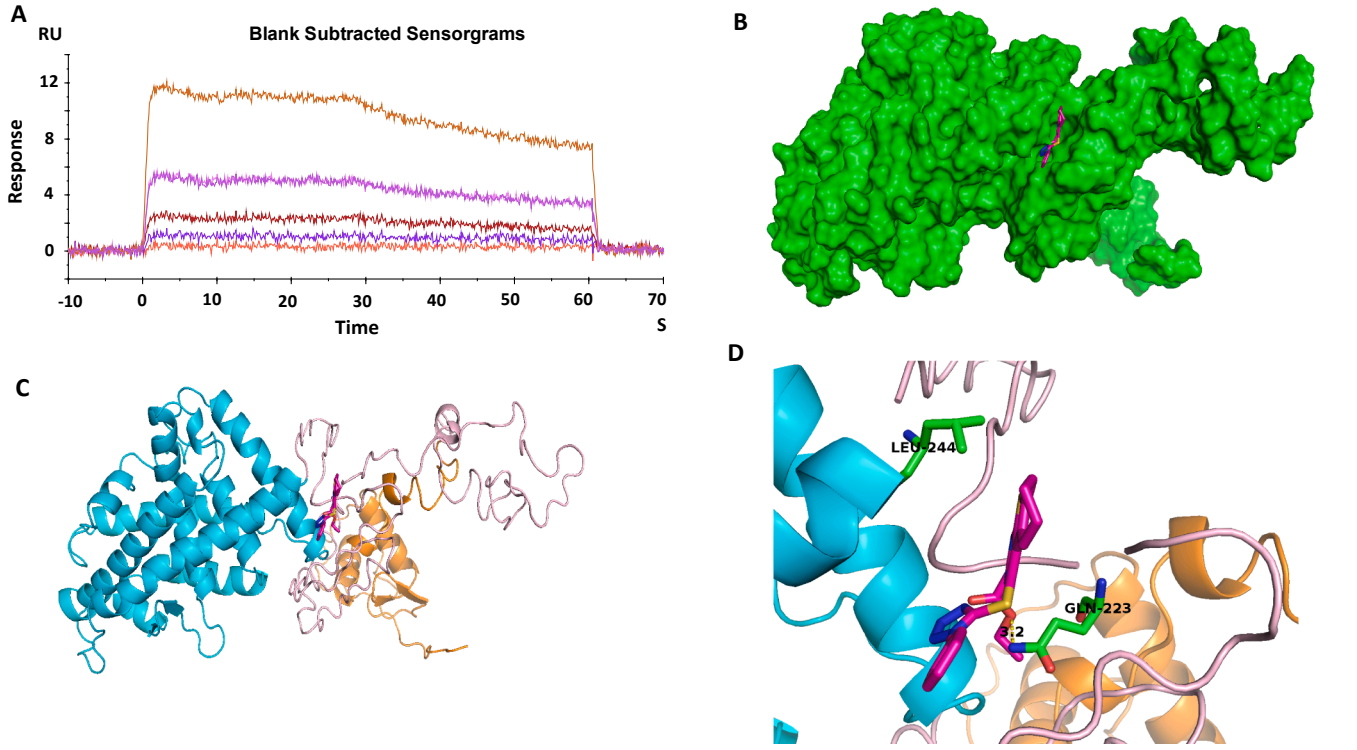

Fig. 3. The binding mechanism studies of compound **28**. (A) Surface plasmon resonance experiment showed compound **28** (10, 5, 2.5, 1.25, 0.625 μM) bound with full-length RORγt protein. (B) The binding pocket of compound **28** (magentas) in RORγt model (green). (C) Compound **28** (magenta) bound in the HD (Green) of RORγt. The DBD (Orange) and LBD (Cyan) were also shown. (D). Compound **28** may form electrostatic interaction and hydrophobic interaction with Gln223 and Leu244 of RORγt respectively.

J = 15.8 Hz, 3H), 2.39–2.28 (m, 1H), 2.08–1.97 (m, 1H), 1.29 (t, J = 7.1 Hz, 3H). ^{13}C NMR (126 MHz, CDCl3) δ 173.90 (s), 167.91 (s), 161.48 (s), 156.26 (s), 146.33 (s), 135.68 (s), 134.15 (s), 130.53 (s), 129.46 (s), 125.36 (d, J = 7.5 Hz), 124.56 (s), 60.99 (s), 39.17 (s), 27.79 (s), 25.54–24.89 (m), 14.23 (s). ESI-MS *m/z*: 453.26 $[M + H]^+$.

Ethyl-2-(4-((1-phenyl-1H-tetrazol-5-yl)thio)-5,6,7,8-tetrahydrobenzo [4,5]thieno[2,3-d]pyrimidin-2-yl)acetate **(28)**. Yield = 63%; ^{1}H NMR (500 MHz, DMSO) δ 7.66 (dd, J = 6.5, 2.8 Hz, 2H), 7.57–7.44 (m, 3H), 3.96 (q, J = 7.1 Hz, 2H), 3.74 (s, 2H), 3.31 (s, 5H), 2.95 (s, 2H), 2.82 (s, 2H), 1.83 (d, J = 4.4 Hz, 4H), 1.10 (t, J = 7.1 Hz, 3H). ^{13}C NMR (126 MHz, $CDCl_3$) δ 169.13 (s), 167.69 (s), 157.44 (s), 156.91 (s), 146.25 (s), 138.85 (s), 133.94 (s), 130.60 (s), 129.49 (s), 126.56 (s), 126.08 (s), 124.93 (s), 61.25 (s), 44.71 (s), 25.91 (d, J = 27.1 Hz), 25.75–25.61 (m), 22.37 (d, J = 11.1 Hz), 14.08 (s). ESI-MS *m/z*: 453.11626 $[M + H]^+$.

3.1.6. Procedure for the preparation of compound *14* and compound *29*

Compound **13** (1.30 mmol) or compound **28** was dissolved in THF (10 mL) and 1 N lithium hydroxide (3.90 mL, 3.90 mmol) was added to it. The mixture was stirred at RT overnight. 1 N HCl was added to the product mixture and extracted with ethyl acetate. The organic phase was washed with brine and the solvent was removed in vacuo. The residue was purified by silica gel chromatography using cyclohexane-acetone(3:1) to give compound **14** or compound **29** (66% yield) as white/yellow solid.

2-Methyl-4-((1-phenyl-1H-tetrazol-5-yl)thio)-5,6,7,8-tetrahydrobenzo [4,5]thieno[2,3-d]pyrimidine-7-carboxylic acid **(14)**. Yield = 49%; ^{1}H NMR (500 MHz, DMSO) δ 12.49 (s, 1H), 7.69 (dd, J = 7.9, 1.7 Hz, 2H), 7.54–7.45 (m, 3H), 3.10–3.01 (m, 2H), 2.94 (dd, J = 16.9, 8.6 Hz, 2H), 2.88–2.78 (m, 1H), 2.35 (s, 3H), 2.24–2.15 (m, 1H), 1.88 (ddd, J = 15.5, 12.5, 7.6 Hz, 1H). ^{13}C NMR (126 MHz, DMSO) δ 175.67 (s), 167.42 (s), 161.25 (s), 156.66 (s), 147.55 (s), 136.37 (s), 134.00 (s), 131.13 (s), 129.98 (s), 125.80 (s), 125.32 (d, J = 27.1 Hz), 38.61 (s), 27.73 (s), 25.24 (d, J = 31.8 Hz), 25.00 (s). ESI-MS *m/z*: 423.17 $[M - H]^-$.

2-(4-((1-Phenyl-1H-tetrazol-5-yl)thio)-5,6,7,8-tetrahydrobenzo[4,5] thieno[2,3-d]pyrimidin-2-yl)acetic acid **(29)**. Yield = 66%; ^{1}H NMR (500 MHz, DMSO) δ 7.64 (d, J = 7.4 Hz, 2H), 7.44 (dt, J = 14.0, 7.0 Hz, 3H), 3.46 (s, 3H), 2.92 (s, 2H), 2.78 (s, 2H), 1.91–1.74 (m, 4H). ^{13}C NMR (126 MHz, DMSO) δ 167.09 (s), 156.53 (s), 147.63 (s), 137.90 (s), 133.81 (s), 131.11 (s), 129.99 (s), 127.11–126.28 (m), 126.21 (s), 126.17–125.23 (m), 26.04 (s), 25.57 (s), 22.31 (d, J = 11.7 Hz). ESI-MS *m/z*: 425.08487 $[M + H]^+$.

3.1.7. Procedure for the preparation of compound *15–25* and compound *30–31*

A mixture of compound **14** or compound **29** (0.28 mmol), aromatic amines derivatives (0.57 mmol), 1-Hydroxybenzotriazole (0.31 mmol) and EDCI (0.31 mmol) was dissolved in Dichloromethane (5 mL). The mixture was stirred at RT overnight. The solvent was removed in vacuo and the residue was extracted with ethyl acetate. Subsequently, the organic layer was washed with brine and the solvent was removed in vacuo. The crude product was purified by silica gel chromatography using cyclohexane-acetone (10:1) to give compound **15–25** or compound **30–31** (42% yield) as white/yellow solid.

2-Methyl-4-((1-phenyl-1H-tetrazol-5-yl)thio)-N-(tetrahydro-2H-pyran-4-yl)-5,6,7,8-tetrahydrobenzo[4,5]thieno[2,3-d]pyrimidine-7-carboxamide **(15)**. Yield = 38%; ^{1}H NMR (500 MHz, DMSO) δ 8.17 (d, J = 8.4 Hz, 1H), 8.01 (d, J = 7.5 Hz, 1H), 7.96 (d, J = 7.5 Hz, 1H), 7.84 (d, J = 8.3 Hz, 1H), 7.72–7.67 (m, 2H), 7.63 (d, J = 8.0 Hz, 1H), 7.51 (d, J = 6.9 Hz, 3H), 3.81 (d, J = 11.0 Hz, 3H), 3.78–3.72 (m, 1H), 3.10 (d, J = 14.9 Hz, 1H), 3.02 (d, J = 5.6 Hz, 1H), 2.91 (s, 3H), 2.72 (d, J = 8.3 Hz, 1H), 2.62 (d, J = 6.0 Hz, 1H), 2.35 (s, 3H), 2.30 (s, 1H), 2.08 (d, J = 10.8 Hz, 2H), 1.80 (d, J = 7.3 Hz, 2H), 1.69 (s, 3H), 1.39 (dd, J = 15.6, 7.2 Hz, 3H), 1.20 (s, 1H). ^{13}C NMR (126 MHz, DMSO) δ 173.16 (s), 167.40 (s), 161.18 (s), 156.60 (s), 147.63 (s), 136.86 (s),

133.98 (s), 131.15 (s), 129.98 (s), 125.69 (s), 125.44 (s), 125.27 (s), 66.35 (s), 45.36 (s), 32.95 (d, J = 8.0 Hz), 28.31 (s), 26.12 (s), 25.43 (d, J = 15.8 Hz). ESI-MS m/z: 530.23 $[M + Na]^+$.

2-Methyl-4-((1-phenyl-1H-tetrazol-5-yl)thio)-N-(m-tolyl)-5,6,7,8-tetrahydrobenzo[4,5]thieno[2,3-d]pyrimidine-7-carboxamide **(16)**. Yield = 66%; ^{1}H NMR (500 MHz, DMSO) δ 9.98 (s, 1H), 7.70 (dd, J = 7.7, 1.8 Hz, 2H), 7.56–7.49 (m, 3H), 7.47 (s, 1H), 7.39 (d, J = 8.2 Hz, 1H), 7.17 (t, J = 7.8 Hz, 1H), 6.85 (d, J = 7.5 Hz, 1H), 3.16 (d, J = 15.7 Hz, 1H), 3.09–2.84 (m, 4H), 2.37 (s, 3H), 2.26 (s, 3H), 2.25–2.19 (m, 1H), 1.96–1.85 (m, 1H). ^{13}C NMR (126 MHz, DMSO) δ 172.87 (s), 167.46 (s), 161.23 (s), 157.27 (s), 156.63 (s), 147.62 (s), 139.57 (s), 138.34 (s), 136.68 (s), 134.02 (s), 131.14 (s), 129.98 (s), 129.01 (s), 125.73 (s), 125.48 (t, J = 25.0 Hz), 124.38 (s), 120.22 (s), 116.86 (s), 28.22 (s), 26.81 (s), 26.08 (s), 25.45 (d, J = 18.5 Hz), 23.76 (s), 21.66 (s). ESI-MS m/z: 514.26 $[M + H]^+$.

N-(4-isopropylphenyl)-2-methyl-4-((1-phenyl-1H-tetrazol-5-yl)thio)-5,6,7,8-tetrahydrobenzo[4,5]thieno[2,3-d]pyrimidine-7-carboxamide **(17)**. Yield = 70%; ^{1}H NMR (500 MHz, DMSO) δ 9.97 (s, 1H), 7.74–7.66 (m, 2H), 7.52 (dd, J = 9.6, 2.6 Hz, 5H), 7.16 (d, J = 8.5 Hz, 2H), 3.16 (d, J = 15.9 Hz, 1H), 3.03 (dd, J = 16.0, 7.3 Hz, 2H), 2.96 (t, J = 8.9 Hz, 1H), 2.90–2.79 (m, 2H), 2.37 (s, 3H), 2.22 (d, J = 13.3 Hz, 1H), 1.95–1.85 (m, 1H), 1.16 (d, J = 6.9 Hz, 6H). ^{13}C NMR (126 MHz, DMSO) δ 172.70 (s), 167.47 (s), 161.23 (s), 156.62 (s), 147.64 (s), 143.76 (s), 137.41 (s), 136.72 (s), 134.01 (s), 131.14 (s), 129.98 (s), 126.87 (s), 125.71 (s), 125.38 (d, J = 16.7 Hz), 119.77 (s), 33.33 (s), 28.26 (s), 26.12 (s), 25.92–25.66 (m), 25.46 (d, J = 21.2 Hz), 24.43 (s). ESI-MS m/z: 542.35 $[M + H]^+$.

N-benzyl-2-methyl-4-((1-phenyl-1H-tetrazol-5-yl)thio)-5,6,7,8-tetrahydrobenzo[4,5]thieno[2,3-d]pyrimidine-7-carboxamide **(18)**. Yield = 44%; ^{1}H NMR (500 MHz, DMSO) δ 8.50 (t, J = 5.9 Hz, 1H), 7.74–7.64 (m, 2H), 7.56–7.47 (m, 3H), 7.31 (t, J = 7.4 Hz, 2H), 7.28–7.19 (m, 3H), 4.33–4.28 (m, 2H), 3.10 (s, 1H), 2.95 (dd, J = 29.7, 23.5 Hz, 3H), 2.81–2.70 (m, 1H), 2.36 (s, 3H), 2.19–2.10 (m, 1H), 1.96–1.78 (m, 1H). ^{13}C NMR (126 MHz, DMSO) δ 129.98 (s), 128.78 (s), 127.59 (s), 125.36 (d, J = 18.6 Hz), 41.40–39.92 (m), 39.74 (d, J = 21.0 Hz), 39.49 (s), 25.42 (d, J = 12.2 Hz). ESI-MS m/z: 514.17 $[M + H]^+$.

N-(3-chlorophenyl)-2-methyl-4-((1-phenyl-1H-tetrazol-5-yl)thio)-5,6,7,8-tetrahydrobenzo[4,5]thieno[2,3-d]pyrimidine-7-carboxamide **(19)**. Yield = 32%; ^{1}H NMR (500 MHz, $CDCl_3$) δ 8.36 (s, 1H), 7.83 (s, 1H), 7.61–7.55 (m, 2H), 7.49 (dd, J = 14.4, 7.9 Hz, 4H), 7.24 (d, J = 8.1 Hz, 1H), 7.09 (d, J = 7.9 Hz, 1H), 3.20 (dd, J = 15.8, 7.3 Hz, 2H), 3.06–2.97 (m, 2H), 2.94 (d, J = 11.1 Hz, 1H), 2.41 (s, 3H), 2.36 (d, J = 6.0 Hz, 1H), 2.06 (dd, J = 12.6, 5.4 Hz, 1H). ^{13}C NMR (126 MHz, $CDCl_3$) δ 172.55 (s), 167.89 (s), 161.41 (s), 155.72 (s), 146.52 (s), 139.19 (s), 136.08 (s), 134.70 (s), 133.92 (s), 130.76 (s), 130.00 (s), 129.58 (s), 125.14 (s), 124.93 (s), 124.48 (s), 120.04 (s), 117.84 (s), 41.76 (s), 28.22 (s), 26.92 (s), 26.27 (s), 25.35 (d, J = 14.7 Hz). ESI-MS m/z: 534.20 $[M + H]^+$.

N-(4-bromophenyl)-2-methyl-4-((1-phenyl-1H-tetrazol-5-yl)thio)-5,6,7,8-tetrahydrobenzo[4,5]thieno[2,3-d]pyrimidine-7-carboxamide **(20)**. Yield = 49%; ^{1}H NMR (500 MHz, DMSO) δ 10.20 (s, 1H), 7.72–7.66 (m, 2H), 7.60 (d, J = 8.9 Hz, 2H), 7.55–7.44 (m, 5H), 5.47 (d, J = 7.5 Hz, 2H), 3.62 (dq, J = 13.1, 6.5 Hz, 2H), 3.16 (d, J = 16.1 Hz, 1H), 3.08–2.84 (m, 4H), 2.37 (s, 3H), 2.23 (dd, J = 10.8, 2.4 Hz, 1H), 1.95–1.85 (m, 1H). ^{13}C NMR (126 MHz, DMSO) δ 173.13 (s), 167.47 (s), 161.25 (s), 157.27 (s), 156.65 (s), 147.63 (s), 139.00 (s), 136.56 (s), 134.01 (s), 132.01 (s), 131.15 (s), 129.98 (s), 125.70 (s), 125.45 (s), 121.58 (s), 115.25 (s), 28.16 (s), 25.99 (s), 25.44 (d, J = 15.3 Hz), 23.76 (s). ESI-MS m/z: 578.09 $[M - H]^-$.

2-Methyl-4-((1-phenyl-1H-tetrazol-5-yl)thio)-N-(thiazol-2-yl)-5,6,7,8-tetrahydrobenzo[4,5]thieno[2,3-d]pyrimidine-7-carboxamide **(21)**. Yield = 43%; ^{1}H NMR (500 MHz, DMSO) δ 12.28 (s, 1H), 7.69 (dd, J = 7.7, 1.8 Hz, 2H), 7.55–7.50 (m, 3H), 7.48 (d, J = 3.5 Hz, 1H), 7.22 (d, J = 3.5 Hz, 1H), 3.18–3.02 (m, 4H), 2.94 (dd, J = 13.8, 6.4 Hz, 1H), 2.37 (s, 3H), 2.24 (d, J = 13.3 Hz, 1H), 1.98–1.89 (m, 1H). ^{13}C NMR (126 MHz, DMSO) δ 172.90 (s), 167.45 (s), 161.30 (s), 158.40 (s), 156.67 (s), 147.63 (s), 138.13 (s), 136.31 (s), 134.00 (s), 131.15 (s), 129.99 (s), 125.71 (s), 125.43 (s), 125.26 (s), 114.02 (s), 31.16 (s), 27.77 (s), 25.81 (s), 25.38 (s). ESI-MS m/z: 507.19 $[M + H]^+$.

2-Methyl-N-(5-methylthiazol-2-yl)-4-((1-phenyl-1H-tetrazol-5-yl)thio)-5,6,7,8-tetrahydrobenzo[4,5]thieno[2,3-d]pyrimidine-7-carboxamide **(22)**. Yield = 20%; ^{1}H NMR (500 MHz, MeOD) δ 7.57 (dt, J = 8.7, 3.9 Hz, 2H), 7.51–7.43 (m, 3H), 7.40 (s, 2H), 7.02 (d, J = 1.1 Hz, 1H), 3.28–3.11 (m, 2H), 3.01 (ddd, J = 30.5, 19.2, 7.3 Hz, 3H), 2.41 (s, 3H), 2.36 (d, J = 0.9 Hz, 3H), 2.30 (dd, J = 16.7, 10.2 Hz, 1H), 2.13–1.99 (m, 1H). ^{13}C NMR (126 MHz, MeOD) δ 133.85 (s), 130.74 (s), 129.53 (s), 124.49 (s), 77.54 (s), 77.40 (d, J = 32.2 Hz), 77.01 (s), 49.18 (s), 49.09–48.65 (m), 48.50 (s), 48.33 (s), 48.15 (s), 40.09 (s), 27.73 (s), 25.77 (s), 25.21 (s), 24.81 (s), 11.20 (s). ESI-MS m/z: 521.25 $[M + H]^+$.

2-Methyl-4-((1-phenyl-1H-tetrazol-5-yl)thio)-N-(pyridin-3-yl)-5,6,7,8-tetrahydrobenzo[4,5]thieno[2,3-d]pyrimidine-7-carboxamide **(23)**. Yield = 38%; ^{1}H NMR (500 MHz, DMSO) δ 10.31 (s, 1H), 8.78 (d, J = 2.3 Hz, 1H), 8.27 (dd, J = 4.6, 1.3 Hz, 1H), 8.08 (ddd, J = 8.3, 2.3, 1.5 Hz, 1H), 7.83–7.66 (m, 2H), 7.62–7.42 (m, 2H), 7.36 (dd, J = 8.2, 4.7 Hz, 1H), 3.26–2.81 (m, 5H), 2.60–2.45 (m, 4H), 2.39 (s, 3H), 2.27 (dd, J = 8.9, 5.0 Hz, 1H), 2.10 (d, J = 16.4 Hz, 1H), 2.03–1.84 (m, 1H). ^{13}C NMR (126 MHz, DMSO) δ 173.71 (s), 167.42 (s), 161.25 (s), 156.66 (s), 147.60 (s), 143.27 (s), 139.63 (s), 136.76 (s), 136.43 (s), 133.98 (s), 131.16 (s), 129.98 (s), 128.16 (s), 125.69 (s), 125.44 (s), 125.24 (s), 124.85 (s), 28.00 (s), 25.93 (s), 25.39 (d, J = 4.8 Hz). ESI-MS m/z: 501.36 $[M + H]^+$.

N-(5-fluoropyridin-2-yl)-2-methyl-4-((1-phenyl-1H-tetrazol-5-yl)thio)-5,6,7,8-tetrahydrobenzo[4,5]thieno[2,3-d]pyrimidine-7-carboxamide **(24)**. Yield = 33%;^{1}H NMR (500 MHz, DMSO) δ 8.34 (d, J = 3.0 Hz, 1H), 8.16 (dd, J = 9.1, 4.1 Hz, 1H), 7.81–7.63 (m, 3H), 7.61–7.46 (m, 3H), 3.14 (t, J = 16.1 Hz, 1H), 3.12–2.85 (m, 4H), 2.38 (s, 3H), 2.31–2.15 (m, 1H), 1.90 (d, J = 7.9 Hz, 1H). ^{13}C NMR (126 MHz, DMSO) δ 173.69 (s), 167.43 (s), 161.25 (s), 156.63 (s), 149.02 (s), 147.63 (s), 136.60 (s), 135.88 (s), 135.68 (s), 133.98 (s), 131.15 (s), 129.99 (s), 125.76 (d, J = 19.8 Hz), 125.44 (s), 125.25 (s), 115.03 (d, J = 3.5 Hz), 27.97 (s), 26.12 (s), 25.46 (d, J = 19.1 Hz). ESI-MS m/z: 519.21 $[M + H]^+$.

N-(6-fluorobenzo[d]thiazol-2-yl)-2-methyl-4-((1-phenyl-1H-tetrazol-5-yl)thio)-5,6,7,8-tetrahydrobenzo[4,5]thieno[2,3-d]pyrimidine-7-carboxamide **(25)**. Yield = 42%; ^{1}H NMR (600 MHz, DMSO) δ 12.59 (s, 1H), 7.93–7.87 (m, 1H), 7.76 (dt, J = 8.9, 4.4 Hz, 1H), 7.74–7.69 (m, 2H), 7.53 (t, J = 1.8 Hz, 3H), 7.29 (ddd, J = 9.2, 7.5, 3.0 Hz, 1H), 3.21–3.02 (m, 4H), 2.98 (dd, J = 16.4, 8.0 Hz, 1H), 2.45 (s, 1H), 2.39 (s, 3H), 2.36–2.27 (m, 1H), 2.09 (s, 1H), 2.02–1.93 (m, 1H), 1.28–1.17 (m, 1H). ^{13}C NMR (126 MHz, DMSO) δ 174.01 (s), 167.41 (s), 161.27 (s), 160.03 (s), 158.34 (s), 158.12 (s), 156.63 (s), 147.59 (s), 145.64 (s), 136.12 (s), 133.99 (s), 133.14 (d, J = 11.0 Hz), 131.13 (s), 129.97 (s), 125.63 (s), 125.42 (s), 125.16 (s), 122.04 (d, J = 8.9 Hz), 114.76 (s), 114.56 (s), 108.96–108.71 (m), 108.57 (d, J = 26.9 Hz), 27.60 (s), 25.69 (s), 25.37 (s). APCI-MS m/z: 574.8 $[M + H]^+$.

N-(5-methylpyridin-2-yl)-2-(4-((1-phenyl-1H-tetrazol-5-yl)thio)-5,6,7,8-tetrahydrobenzo[4,5]thieno[2,3-d]pyrimidin-2-yl)acetamide **(30)** Yield = 59%; ^{1}H NMR (500 MHz, DMSO) δ 8.14 (d, J = 1.3 Hz, 1H), 7.92–7.82 (m, 1H), 7.66 (d, J = 7.6 Hz, 2H), 7.57 (dd, J = 8.5, 2.0 Hz, 1H), 7.47 (d, J = 7.4 Hz, 1H), 7.41 (t, J = 7.6 Hz, 2H), 3.83 (s, 2H), 2.95 (s, 2H), 2.82 (s, 3H), 2.73–2.65 (m, 1H), 2.29 (s, 1H), 2.23 (s, 3H), 1.83 (d, J = 4.9 Hz, 4H). ^{13}C NMR (126 MHz, DMSO) δ 163.55 (s), 158.95 (s), 154.66 (s), 131.20 (s), 130.96 (s), 120.62 (s), 25.73 (s), 24.82 (s), 22.99 (s), 22.26 (s), 21.28 (s). ESI-MS m/z: 515.14344 $[M + H]^+$.

N-(5-methylpyridin-2-yl)-2-(4-((1-phenyl-1H-tetrazol-5-yl)thio)-5,6,7,8-tetrahydrobenzo[4,5]thieno[2,3-d]pyrimidin-2-yl)acetamide **(31)** Yield = 29%; ^{1}H NMR (500 MHz, DMSO) δ 7.72–7.65 (m, 2H), 7.54–7.33 (m, 5H), 7.12–7.02 (m, 2H), 3.93–3.86 (m, 2H), 3.00–2.90 (m, 2H), 2.86–2.79 (m, 2H), 1.88–1.75 (m, 4H). ^{13}C NMR (126 MHz, DMSO) δ 167.12 (s), 158.96 (s), 158.61 (s), 157.32 (s), 154.68 (s), 147.37 (s), 138.89 (s), 133.86 (s), 131.10 (t, J = 15.5 Hz), 129.86 (s), 128.03–126.57 (m), 126.44 (s), 125.97 (d, J = 59.1 Hz), 121.54 (s),

31.62 (s), 30.29 (s), 29.47 (s), 29.16 (s), 26.05 (s), 25.82–24.54 (m), 22.99 (s), 22.29 (d, J = 6.9 Hz), 21.29 (s). ESI-MS m/z: 540.13865 $[M + H]^+$.

3.2. SPR

Retinoid-related orphan receptor gamma-t (RORγt) protein was immobilized on a CM5 Sensor Chip (carboxymethylated dextran covalently attached to a gold surface) with an amine coupling kit from GE Healthcare. The RORγt protein was pre-incubated with different concentration of compound **28** (10, 5, 2.5, 1.25, 0.625 μM) had well binding with full-length RORγt protein in a PBS buffer (10 mM) with 1% DMSO. The signals were recorded with a BiacoreT100 instrument with the standard protocol.

3.3. Molecular docking

The model of full-length human RORγt was built with I-Tasser (id S428560) [36]. The ligand prepared with Ligandscout (4.1) with MMFF 94 energy minimization of compound **28**. Then the whole protein model was selected for docking and the prepared molecules were inserted. The docking was carried out by AutoDock Vina 1.1 (Exhaustiveness = 20, Max. Energy difference = 3).

3.4. Biology

3.4.1. Generals

All animal experiments were approved by Ethics Committee of ZSSOM on Laboratory Animal Care (No. 2017-273) and were performed according to the guidelines of the Institute for Laboratory Animal Research of Sun Yat-sen University Laboratory Animal Center (Guangzhou, China).

Data are expressed as mean ± SEM. The statistical significance between groups was determined by Student's t test. $p < 0.05$ was considered to be statistically significant. Statistical analyses were performed using GraphPad Prism 5.0 (GraphPad Software Inc., San Diego, CA, USA)

3.4.2. Mice

We used 5–6 weeks old C57BL/6J female mice for T cell differentiation *in vitro* experiments. All of the animals were purchased from the National Resource Center for Mutant Mice of China (Nanjing, China).

3.4.3. T cell differentiation in vitro

$CD4^+CD25^-$ T cells were purified using a MACS magnetic column with a CD4+ T cell negative enrichment kit according to the manufacturer's protocol (eBioscience, USA). Native CD4 T cell were activated with anti-CD3e antibody (5 μg/mL, eBioscience) and anti-CD28 antibody (2 μg/mL, eBioscience) in 12-well plates. Cultures were supplemented with mouse IL-6 (30 ng/mL, R&D Systems, Minneapolis, MN, USA); human TGF-β (5 ng/mL, R&D Systems); mouseIL-1β (20 ng/mL, R&D Systems); anti-mouse-IL-4 antibody (5 μg/mL, eBioscience); and anti-mouse-IFN-γ antibody (5 μg/mL, eBioscience).

3.4.4. EC_{50} assay – luciferase reporter assays

PGL4.31 + hRORγt + Jurkatcells (4×10^5/mL) were seeded into 96-well round-bottom plates and cultured with these five compounds **6, 10, 22, 28, 31** (0.15, 0.31, 0.62, 1.25, 2.50, 10.00 μM). Cells were lysed 6 h later and the half-maximal effective concentrations (EC_{50}) were determined.

3.4.5. CC_{50} assay – cell viability assays

PGL4.31 + hRORγt + Jurkat cells (2×10^5/mL) were seeded into 96-well round-bottom plates and cultured with these five compounds **6, 10, 22, 28, 31** (0.15, 0.31, 0.62, 1.25, 2.50, 10.00 μM). After 48 h, MTT (dimethylthiazolyl-2–5-diphenyltetrazoliumbromide) was added and incubated at 37 °C for 4 h, and then the supernatant was discarded. The Optical density (OD) was then measured at 495 nm.

3.4.6. Flow cytometry

The fluorochrome-labeled antibodies were used in following: Percific Blue anti-mouse-CD4 (eBioscience), PE anti-mouse-TCR-β (BD Biosciences) and APC anti-mouse- IL-17A (eBioscience). Data analysed by FlowJo software.

3.4.7. RNA isolation and quantitative RT-PCR

Total RNA from spleen were extracted using Trizol reagent (Invitrogen). Amounts of 1 μg were reverse-transcribed into cDNA using the PrimeScript RT Reagent Kit (Takara Bio, Kusatsu, Japan). Gene expression was determined using the Quantitative Real-Time PCR technique (Takara Bio, Kusatsu, Japan). The relative expression was calculated by normalizing the expression of each target to glyceraldehyde-3-phosphate dehydrogenase (GAPDH) using the 2-ΔΔCt method. The primers was used in Quantitative RT-PCR in following: *GAPDH*, forward sequence: TGGTGAAGGTCGGTGTGAAC, reverse sequence: CCATGTAGTTGAGGTCAATGAAGG; *RORγt,* forward sequence: AAACTTGACAGCATCTCGGGA, reverse sequence: TGCAGGAGTAGGC CACATTACA; *IL-17A*, forward sequence: CTCCAGAAGGCCCTCAGAC TAC, reverse sequence: AGCTTTCCCTCCGCATTGACACAG; *IL-17F*, forward sequence: GAGGATAACACTGTGAGAGTTGAC, reverse sequence: GAGTTCATGGTGCTGTCTTCC.

4. Conclusions

The important roles of RORγt in the differentiation of Th17 cells have made it a promising target to develop therapeutics for autoimmune diseases. Most of the current research has been focused on LBD of RORγt and discovered potent inhibitors and agonists. Recent reports showed that the mutations on amino acids of HD and DBD of RORγt could obviously inhibit Th17 differentiation with little effect on thymocyte development. These results discovered that HD has vital involvement on RORγt's function which has not been considered adequately. Thereof, the potential of full-length RORγt to develop potent RORγt inhibitors should be studied. In this work, we performed SAR studies of 5,6,7,8-tetrahydrobenzo[4,5]thieno[2,3-*d*]pyrimidine derivatives with a screening system utilizing full-length RORγt. We then discovered compounds with potent activities to inhibit Th17 differentiation and Th17 cytokine production without obvious effects on thymocyte apoptosis. The SPR and molecular docking studies showed that compound **28** may bind in the hinge domain of RORγt. Our studies shed lights on the possibilities of utilizing full-length RORγt to develop novel RORγt inhibitors with more potency and specificity.

Acknowledgments

This work was supported by the grants from National Natural Science Foundation of China (21572281, 21877132), Scientific Plan of Guangzhou City (201704030087), Scientific Plan of Guangdong Province (2017A020211003) to C.B. This research was supported by Science and Technology Department of Guangdong Province (2017A050501010 and 2016A050503023), and Guangzhou Science Technology and Innovation Commission (201807010042) to Z.H.

Declaration of Competing Interest

The authors declare no conflict of interest.

Appendix A. Supplementary material

Supplementary data to this article can be found online at https://doi.org/10.1016/j.bioorg.2019.103077.

References

[1] I.I. Ivanov, B.S. McKenzie, L. Zhou, C.E. Tadokoro, A. Lepelley, J.J. Lafaille, D.J. Cua, D.R. Littman, The orphan nuclear receptor ROR gamma t directs the differentiation program of proinflammatory IL-17(+) T helper cells, Cell 126 (6) (2006) 1121–1133.

[2] S.L. Gaffen, R. Jain, A.V. Garg, D.J. Cua, The IL-23-IL-17 immune axis: from mechanisms to therapeutic testing, Nat. Rev. Immunol. 14 (9) (2014) 585–600.

[3] L. Codarri, G. Gyulveszi, V. Tosevski, L. Hesske, A. Fontana, L. Magnenat, T. Suter, B. Becher, ROR gamma t drives production of the cytokine GM-CSF in helper T cells, which is essential for the effector phase of autoimmune neuroinflammation, Nat. Immunol. 12 (6) (2011) 560–U248.

[4] T.P. Burris, S.A. Busby, P.R. Griffin, Targeting orphan nuclear receptors for treatment of metabolic diseases and autoimmunity, Chem. Biol. 19 (1) (2012) 51–59.

[5] J.F. Yang, M.S. Sundrud, J. Skepner, T. Yamagata, Targeting Th17 cells in autoimmune diseases, Trends Pharmacol. Sci. 35 (10) (2014) 493–500.

[6] P. Miossec, J.K. Kolls, Targeting IL-17 and TH17 cells in chronic inflammation, Nat. Rev. Drug Discov. 11 (10) (2012) 763–776.

[7] D.R. Withers, M.R. Hepworth, X. Wang, E.C. Mackley, E.E. Halford, E.E. Dutton, C.L. Marriott, V. Brucklacher-Waldert, M. Veldhoen, J. Kelsen, R.N. Baldassano, G.F. Sonnenberg, Transient inhibition of ROR-gammat therapeutically limits intestinal inflammation by reducing TH17 cells and preserving group 3 innate lymphoid cells, Nat. Med. 22 (3) (2016) 319–323.

[8] V.B. Pandya, S. Kumar, R. Sachchidanand, R.C. Desai Sharma, Combating autoimmune diseases with retinoic acid receptor-related orphan receptor-gamma (ROR gamma or RORc) inhibitors: hits and misses, J. Med. Chem. 61 (24) (2018) 10976–10995.

[9] D.A. Carcache, A. Vulpetti, J. Kallen, H. Mattes, D. Orain, R. Stringer, E. Vangrevelinghe, R.M. Wolf, K. Kaupmann, J. Ottl, J. Dawson, N.G. Cooke, K. Hoegenauer, A. Billich, J. Wagner, C. Guntermann, S. Hintermann, Optimizing a weakly binding fragment into a potent ROR gamma t inverse agonist with efficacy in an in vivo inflammation model, J. Med. Chem. 61 (15) (2018) 6724–6735.

[10] K. Venken, P. Jacques, C. Mortier, M.E. Labadia, T. Decruy, J. Coudenys, K. Hoyt, A.L. Wayne, R. Hughes, M. Turner, S. Van Gassen, L. Martens, D. Smith, C. Harcken, J. Wahle, C.T. Wang, E. Verheugen, N. Schryvers, G. Varkas, H. Cypers, R. Wittoek, Y. Piette, L. Gyselbrecht, S. Van Calenbergh, F. Van den Bosch, Y. Saeys, G. Nabozny, D. Elewaut, ROR gamma t inhibition selectively targets IL-17 producing iNKT and gamma delta-T cells enriched in Spondyloarthritis patients, Nat. Commun. 10 (2019).

[11] P. Cyr, S.M. Bronner, J.J. Crawford, Recent progress on nuclear receptor ROR gamma modulators, Bioorg. Med. Chem. Lett. 26 (18) (2016) 4387–4393.

[12] Y. Zhang, X.Y. Luo, D.H. Wu, Y. Xu, ROR nuclear receptors: structures, related diseases, and drug discovery (vol 36, pg 71, 2015), Acta Pharmacol. Sin. 36 (2) (2015) 290.

[13] J.R. Huh, D.R. Littman, Small molecule inhibitors of ROR gamma t: Targeting Th17 cells and other applications, Eur. J. Immunol. 42 (9) (2012) 2232–2237.

[14] S.M. Bronner, J.R. Zbieg, J.J. Crawford, ROR gamma antagonists and inverse agonists: a patent review, Expert Opin. Ther. Pat. 27 (1) (2017) 101–112.

[15] T. Yang, Q. Liu, Y.B. Cheng, W. Cai, Y.L. Ma, L.Q. Yang, Q.Q. Wu, L.A. Orband-Miller, L. Zhou, Z.J. Xiang, M. Huxdorf, W. Zhang, J. Zhang, J.N. Xiang, S. Leung, Y. Qiu, Z. Zhong, J.D. Elliott, X.C. Lin, Y.H. Wang, Discovery of tertiary amine and indole derivatives as potent ROR gamma t inverse agonists, ACS Med. Chem. Lett. 5 (1) (2014) 65–68.

[16] W. Zhang, J. Zhang, L.P. Fang, L. Zhou, S. Wang, Z.J. Xiang, Y. Li, B. Wisely, G.F. Zhang, G. An, Y.H. Wang, S. Leung, Z. Zhong, Increasing human Th17 differentiation through activation of orphan nuclear receptor retinoid acid-related orphan receptor gamma (ROR gamma) by a class of aryl amide compounds, Mol. Pharmacol. 82 (4) (2012) 583–590.

[17] K. Hirata, M. Kotoku, N. Seki, T. Maeba, K. Maeda, S. Hirashima, T. Sakai, S. Obika, A. Hori, Y. Hase, T. Yamaguchi, Y. Katsuda, T. Hata, N. Miyagawa, K. Arita, Y. Nomura, K. Asahina, Y. Aratsu, M. Kamada, T. Adachi, M. Noguchi, S. Doi, P. Crowe, E. Bradley, R. Steensma, H. Tao, M. Fenn, R. Babine, X. Li, S. Thacher, H. Hashimoto, M. Shiozaki, SAR exploration guided by LE and Fsp(3): discovery of a selective and orally efficacious RORgamma inhibitor, ACS Med. Chem. Lett. 7 (1) (2016) 23–27.

[18] B.P. Fauber, O. Rene, Y.Z. Deng, J. DeVoss, C. Eidenschenk, C. Everett, A. Ganguli, A. Gobbi, J. Hawkins, A.R. Johnson, H. La, J. Lesch, P. Lockey, M. Norman, W.J. Ouyang, S. Summerhill, H. Wong, Discovery of 1-{4-[3-Fluoro-4-((3S,6R)-3-methyl-1,1-dioxo-6-phenyl-[1,2]thiazinan-2-ylmethyl)-phenyl]-piperazin-1-yl}-ethanone (GNE-3500): a potent, selective, and orally bioavailable retinoic acid receptor-related orphan receptor C (RORc or ROR gamma) inverse agonist, J. Med. Chem. 58 (13) (2015) 5308–5322.

[19] Y.H. Wang, W. Cai, Y.B. Cheng, T. Yang, Q. Liu, G.F. Zhang, Q.H. Meng, F.B. Han, Y.F. Huang, L. Zhou, Z.J. Xiang, Y.G. Zhao, Y. Xu, Z.Q. Cheng, S.J. Lu, Q.Q. Wu, J.N. Xiang, J.D. Elliott, S. Leung, F. Ren, X.C. Lin, Discovery of Biaryl amides as potent orally bioavailable, and CNS penetrant ROR gamma t inhibitors, ACS Med. Chem. Lett. 6 (7) (2015) 787–792.

[20] F. Narjes, Y.F. Xue, S. von Berg, J. Malmberg, A. Llinas, R.I. Olsson, J. Jirholt, H. Grindebacke, A. Leffler, N. Hossain, M. Lepisto, L. Thunberg, H. Leek, A. Aagaard, J. McPheat, E.L. Hansson, E. Back, S. Tangefjord, R.F. Chen, X. Yao, H.B. Ge, T.G. Hansson, Potent and orally bioavailable inverse agonists of ROR gamma t resulting from structure-based design, J. Med. Chem. 61 (17) (2018) 7796–7813.

[21] Y. Zhang, X. Wu, X. Xue, C. Li, J. Wang, R. Wang, C. Zhang, C. Wang, Y. Shi, L. Zou, Q. Li, Z. Huang, X. Hao, K. Loomes, D. Wu, H.W. Chen, J. Xu, Y. Xu, Discovery and characterization of XY101, a potent, selective, and orally bioavailable RORgamma inverse agonist for treatment of castration-resistant prostate cancer, J. Med. Chem. 62 (9) (2019) 4716–4730.

[22] M. Kotoku, T. Maeba, S. Fujioka, M. Yokota, N. Seki, K. Ito, Y. Suwa, T. Ikenogami, K. Hirata, Y. Hase, Y. Katsuda, N. Miyagawa, K. Arita, K. Asahina, M. Noguchi, A. Nomura, S. Doi, T. Adachi, P. Crowe, H. Tao, S. Thacher, H. Hashimoto, T. Suzuki, M. Shiozaki, Discovery of second generation RORgamma inhibitors composed of an azole scaffold, J. Med. Chem. 62 (5) (2019) 2837–2842.

[23] S. Fujita-Sato, S. Ito, T. Isobe, T. Ohyama, K. Wakabayashi, K. Morishita, O. Ando, F. Isono, Structural basis of digoxin that antagonizes ROR gamma t receptor activity and suppresses Th17 cell differentiation and interleukin (IL)-17 production, J. Biol. Chem. 286 (36) (2011) 31409–31417.

[24] N. Gallastegui, J.A.G. Mackinnon, R.J. Fletterick, E. Estebanez-Perpina, Advances in our structural understanding of orphan nuclear receptors, Trends Biochem. Sci. 40 (1) (2015) 25–35.

[25] O. Rene, B.P. Fauber, G.D. Boenig, B. Burton, C. Eidenschenk, C. Everett, A. Gobbi, S.G. Hymowitz, A.R. Johnson, J.R. Kiefer, M. Liimatta, P. Lockey, M. Norman, W.J. Ouyang, H.A. Wallweber, H. Wong, Minor Structural change to tertiary sulfonamide RORc ligands led to opposite mechanisms of action, ACS Med. Chem. Lett. 6 (3) (2015) 276–281.

[26] S. Xiao, N. Yosef, J. Yang, Y. Wang, L. Zhou, C. Zhu, C. Wu, E. Baloglu, D. Schmidt, R. Ramesh, M. Lobera, M.S. Sundrud, P.Y. Tsai, Z. Xiang, J. Wang, Y. Xu, X. Lin, K. Kretschmer, P.B. Rahl, R.A. Young, Z. Zhong, D.A. Hafler, A. Regev, S. Ghosh, A. Marson, V.K. Kuchroo, Small-molecule RORgammat antagonists inhibit T helper 17 cell transcriptional network by divergent mechanisms, Immunity 40 (4) (2014) 477–489.

[27] M. Scheepstra, S. Leysen, G.C. van Almen, J.R. Miller, J. Piesvaux, V. Kutilek, H. van Eenennaam, H.J. Zhang, K. Barr, S. Nagpal, S.M. Soisson, M. Kornienko, K. Wiley, N. Elsen, S. Sharma, C.C. Correll, B.W. Trotter, M. van der Stelt, A. Oubrie, C. Ottmann, G. Parthasarathy, L. Brunsveld, Identification of an allosteric binding site for ROR gamma t inhibition, Nat. Commun. 6 (2015).

[28] Z.M. Sun, D. Unutmaz, Y.R. Zou, M.J. Sunshine, A. Pierani, S. Brenner-Morton, R.E. Mebius, D.R. Littman, Requirement for ROR gamma in thymocyte survival and lymphoid organ development, Science 288 (5475) (2000) 2369–2373.

[29] E. Ueda, S. Kurebayashi, M. Sakaue, M. Backlund, B. Koller, A.M. Jetten, High incidence of T-cell lymphomas in mice deficient in the retinoid-related orphan receptor ROR gamma, Cancer Res. 62 (3) (2002) 901–909.

[30] S. Kurebayashi, E. Ueda, M. Sakaue, D.D. Patel, A. Medvedev, F. Zhang, A.M. Jetten, Retinoid-related orphan receptor gamma (ROR gamma) is essential for lymphoid organogenesis and controls apoptosis during thymopoiesis, Proc. Natl. Acad. Sci. USA 97 (18) (2000) 10132–10137.

[31] G. Eberl, S. Marmon, M.J. Sunshine, P.D. Rennert, Y.W. Choi, D.R. Littman, An essential function for the nuclear receptor ROR gamma t in the generation of fetal lymphoid tissue inducer cells, Nat. Immunol. 5 (1) (2004) 64–73.

[32] Z.H. He, J. Ma, R.Q. Wang, J. Zhang, Z.F. Huang, F. Wang, S. Sen, E.V. Rothenberg, Z.M. Sun, A two-amino-acid substitution in the transcription factor ROR gamma(g)t disrupts its function in T(H)17 differentiation but not in thymocyte development, Nat. Immunol. 18 (10) (2017) 1128.

[33] Z. He, J. Zhang, Z. Huang, Q. Du, N. Li, Q. Zhang, Y. Chen, Z. Sun, Sumoylation of RORgammat regulates TH17 differentiation and thymocyte development, Nat. Commun. 9 (1) (2018) 4870.

[34] Q. Ding, M. Zhao, C. Bai, B. Yu, Z. Huang, Inhibition of RORgammat activity and Th17 differentiation by a set of novel compounds, BMC Immunol. 16 (2015) 32.

[35] Q.F. Ding, M. Zhao, B.L. Yu, C. Bai, Z.F. Huang, Identification of tetraazacyclic compounds as novel potent inhibitors antagonizing ROR gamma t activity and suppressing Th17 cell differentiation, PLoS ONE 10 (9) (2015).

[36] A. Roy, A. Kucukural, Y. Zhang, I-TASSER: a unified platform for automated protein structure and function prediction, Nat. Protoc. 5 (4) (2010) 725–738.